Applied Thermal Engineering 215 (2022) 118991

Contents lists available at ScienceDirect

Applied Thermal Engineering

journal homepage: www.elsevier.com/locate/apthermeng

Impact of an internal heat exchanger on a transcritical CO_2 heat pump under optimal pressure conditions
Optimal-pressure performance of CO_2 heat pump with IHX

Ramón A. Otón-Martínez [b,*], Fernando Illán-Gómez [a], José R. García-Cascales [a], F.J.S. Velasco [a], M. Reda Haddouche [a]

[a] Department of Thermal and Fluid Engineering, Universidad Politécnica de Cartagena, 30202 Cartagena, Spain
[b] Centro Universitario de la Defensa, Universidad Politécnica de Cartagena, C/ Coronel López Peña S/N, Base Aérea de San Javier, Santiago de La Ribera, 30720 Murcia, Spain

ARTICLE INFO

Keywords:
CO_2 heat hump
R744
Space heating
Internal heat exchanger
Hot water generation
Optimal pressure

ABSTRACT

Transcritical R744 (CO_2) heat pumps are a low-GWP high-efficiency alternative for domestic hot water generation and space heating. For high set-point temperatures, however, the COP drops and the optimum operating pressure increases. For this reason, the effect on system performance achieved by the inclusion of an Intermediate Heat Exchanger (IHX) is analyzed in depth. This is carried out by means of a numerical-experimental approach in which the effectiveness of the IHX and other characteristic parameters of the heat pump cycle are studied as a function of the IHX heat transfer area. The numerical modeling of the heat pump components is implemented for transient simulations of system heating-up process. Experimental tests with and without IHX are carried out with a water-to-water heat pump that feeds an accumulator tank, to assess its influence on the system's COP and the electrical consumption. Simulations reveal that improving the efficiency of the IHX, by increasing the exchange area, improves the system's performance. For the cases with higher IHX exchange area, the optimum pressure in the system is lower. For the heating experiments, the resulting thermodynamic COP is 7.55 % higher in the case with IHX, while the effective COP increases by 4.26 %. In consequence, the use of the IHX is recommended for the conditions analyzed.

1. Introduction

Many technical solutions are currently available on the market for the generation of domestic hot water (DHW) and space heating, among which, probably, one of the most energy efficient is the use of water-water heat pumps. The use of heat pumps for heating homes and other urban buildings, instead of gas or diesel boilers, also has the advantage of reducing localized emissions in highly populated urban areas, which contributes to improving air quality in cities. Multiple domestic heat pump models are currently marketed by different companies, but most available models use hydrofluorocarbon refrigerants (HFCs). These refrigerants, which are the most common in domestic and industrial applications, are being viewed with increasing concern by the authorities and society as a whole, due to the environmental implications of their use, related to their high global warming potential (GWP).

As an alternative to HFC refrigerants, the R744 (CO_2) refrigerant has made a major resurgence in the last twenty years. Carbon dioxide had been a traditionally used refrigerant at the beginning of the twentieth century, put aside for decades due to technical disadvantages, such as high working pressures, and it has been retaken, especially since the 1990s [1], due to its multiple advantages: it is a natural fluid, non-flammable, it is not toxic to humans, with a GWP of 1 and ODP equal to zero, and it shows high heat transfer coefficients in the supercritical region.

However, due to the thermodynamic properties of CO_2 (its critical temperature is 31.03 °C), for the usual application conditions of heat pumps for DHW, CO_2 will work in a transcritical cycle. The thermodynamic efficiency of transcritical CO_2 cycles depends to a great extent on the working conditions, but is generally lower than the efficiency obtained with HFCs in sub-critical cycles [2]. However, when a transcritical CO_2 heat pump is required to provide a high rise in temperature

* Corresponding author.
E-mail addresses: ramon.oton@cud.upct.es (R.A. Otón-Martínez), fernando.illan@upct.es (F. Illán-Gómez), jr.garcia@upct.es (J.R. García-Cascales), fjavier.sanchez@upct.es (F.J.S. Velasco), mohammedreda.haddouche@edu.upct.es (M. Reda Haddouche).

https://doi.org/10.1016/j.applthermaleng.2022.118991
Received 18 February 2022; Received in revised form 17 June 2022; Accepted 6 July 2022
Available online 16 July 2022

Nomenclature

Acronyms

BPV	back pressure valve
COP	coefficient of performance
DHW	domestic hot water
DMS	dedicated mechanical subcooling
EEV	electronic expansion valve
GWP	global warming potential
IHX	intermediate heat exchanger
ODP	ozone depletion potential

Variables

A_{calc}	calculated heat transfer area (m^2)
A_0	actual heat transfer area (m^2)
h	specific enthalpy ($kJ \cdot kg^{-1}$)
$\dot{m}$	mass flow rate ($kg \cdot s^{-1}$)
M	mass
P	pressure (MPa, Pa, bars depending on the case)
Q	heat transferred (kJ or kWh depending on the case)
$\dot{Q}$	heat transferred per unit time (kW)
T	temperature (°C)
W	compressor work (kJ)
$\dot{W}$	compressor work per unit time (kW)
ε	effectiveness
ρ	density ($kg \cdot m^{-3}$)
Δ	difference

Subscripts

a	compressor suction
c	cold
c	compressor
comp	compressor
eff	effective
elec	electric
ev	evaporation
evap	evaporator
exp	experimental
gc	gas cooler
h	hot
HP	high pressure
i	inlet
in	inlet
LP	low pressure
max	maximum
o	outlet
out	outlet
opt	optimal
r	refrigerant
tank	tank
w	water

of the water in the gas cooler, the COP of the system is usually higher than that of a conventional heat pump [3]. Even so, in DHW installations the hot water is usually discharged into a stratified tank. In this case, the temperature set point is usually constant (for example, around 60 °C) and, as the tank heats up, the water returns to the cooler gas at a higher temperature. The difference in water temperatures is reduced as well as the efficiency of the system [4], while the optimum working pressure increases.

Different methods can be considered to improve the COP of a CO_2 transcritical cycle, both in the heating and the refrigeration cycle, in most cases focused on achieving a certain level of subcooling at the gas cooler outlet. One of the most investigated techniques is Dedicated Mechanical Subcooling (DMS) [5,6]. D'Agaro et al. [6] show a great effectiveness of DMS when compared with other alternatives. However, the DMS increases the cost and complexity of the installation to the point of making it unfeasible for small domestic equipment or mobile systems, such as those used in the automotive industry. Exploring a different option, Aranguren et al. [7] used thermoelectric subcooler, achieving an experimental COP improvement of 11.3 % and increasing the cooling capacity in a refrigeration cycle. Finally, an option that arouses great interest is the addition of an Internal Heat Exchanger (IHX), which uses the refrigerant at the evaporator outlet for subcooling at the gas cooler outlet, achieving a pressure drop in the system [8–13].

In this regard, Calabrese et al. [9] studied an air-to-air CO_2 heat pump with IHX, confirming that the best COP values are obtained in low-temperature working conditions. For a CO_2 refrigeration system, Chen and Gu [10] provided a new expression for the effectiveness of the heat exchanger and studied by means of simulations the influence of IHX effectiveness and the ambient temperature, as well as the IHX inlet quality in the optimal operating pressure. In higher power equipment, for example, for refrigeration applications in supermarkets, the use of IHX has also been proposed in combination with parallel compressor and ejector expansion devices [11].

In the design of a heat pump with IHX, it is essential to know the influence of the exchange area of the IHX on the performance of the system. Cho et al. [12] investigated the influence of the length of an IHX on the cooling performance of a variable speed CO_2 cycle. This was a double-tube heat exchanger, whose length was varied from 0 to 3 m, achieving an increase in COP between 7 and 9 %. Increasing the size of the IHX can contribute to reducing the optimal discharge pressure and this reduces the throttling valve irreversibility, which improves the exergy efficiency, as shown by Wang et al. [14] in an exergo-economic evaluation. In this sense, Kim at al. [15] have shown that an increase in COP can be achieved by increasing the length of the IHX, when counter-flow heat exchangers with concentric dual copper tubes are used, although the corresponding pressure drop decreases the heating capacity.

However, for a compact heat pump system suitable for residential use, it is important that each of the system components be small in size. A good option for a compact IHX that allows high working pressures is a plate heat exchanger. Despite the extensive literature on IHX in CO_2 refrigeration systems, there is a lack of information on the correct sizing of these exchangers. Fang et al. [13] used an aluminum plate IHX in an experimental study and reported the exergy analysis of a refrigeration system for automotive applications. The size of the IHX was evaluated only by the effectiveness of the heat exchanger, not by the variation of the heat exchange area. To the authors' knowledge, no works are found in the literature that evaluate the influence of the IHX area for a plate exchanger in CO_2 heat pumps. In addition, while most of the existing works analyze the influence of the IHX under stationary operating conditions, this work analyzes it under real operating conditions during the entire heating process, from the start of the installation to its shut-down, with the objective of demonstrating that for the entire range of operating conditions the IHX improves the efficiency of the system. Thus, the study presented here is dedicated to increasing the existing knowledge about the influence that the characteristics of the IHX have on the performance of the system when it is applied to the heating process of a hot water tank. Concretely, this paper focusses in the study of a brazed plate IHX integrated in a transcritical CO_2 heat pump that operates with a dry expansion evaporator and a liquid receiver placed

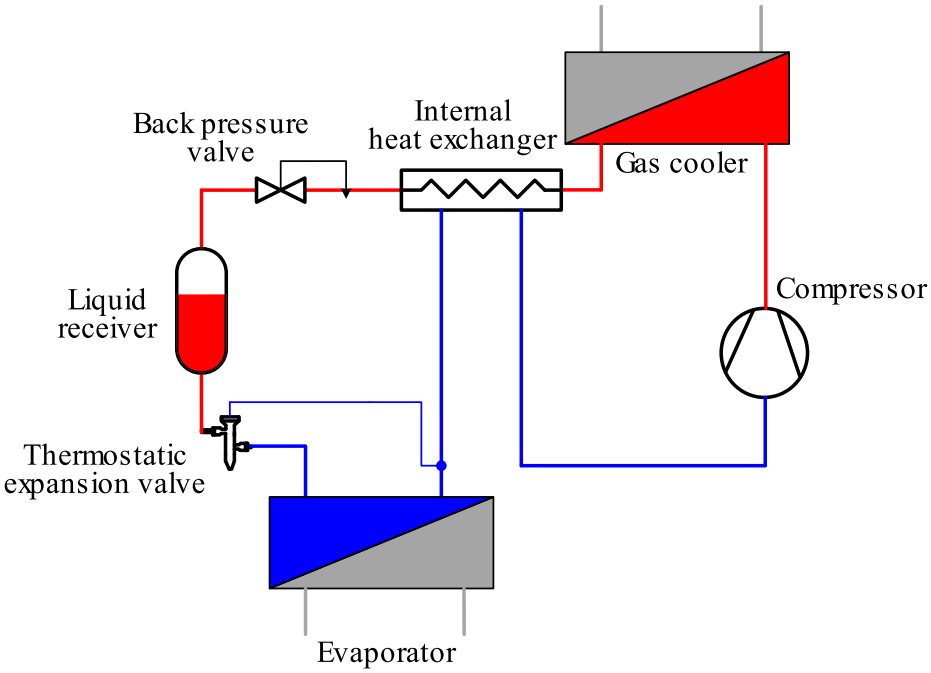

Fig. 1. Sketch of the system studied.

Table 1
Components of the experimental heat pump (manufacturer and model).

Equipment	Manufacturer	Model	Tech. info
Compressor	Dorin	CD300H	$\dot{V} = 1.46 m^3/h$
Evaporator	Swep	B8Tx26P	$A = 0.552\ m^2$
Gas cooler	Swep	B16x34P	$A = 1.31\ m^2$
Liquid to vapour heat exchanger	Swep	B17x4P	$A = 0.082\ m^2$
Back pressure expansion valve	Carel	E2V11CS100	$Kv = 0.042\ m^3/h$
Thermostatic expansion valve	Carel	E2V24CS100	$Kv = 0.18\ m^3/h$

Table 2
Main geometrical data of the IHX according to the manufacturer.

Number of plates	Height (m)	Width (m)	Pitch (mm)	Heat transfer area (m^2)	Corrugation angle
4	0.377	0.1195	2	0.082	120°
Channels according to the fluid:			2 channels high pressure side, 1 channel low pressure side.		

before the evaporator.

2. Materials and methods

2.1. Heat pump experimental set-up

In what follows, the experimental equipment is presented, making a description of the system and each of its components, as well as the experimental methodology that has been followed in carrying out the tests. A water-water heat pump has been used, which works in a transcritical cycle with CO_2 refrigerant. The installation, which has been dimensioned to meet a heating capacity of 8 kW, has been developed and studied in previous works by this research group [16]. It is a complex and multipurpose facility that allows studying multiple configurations, depending on the chosen set-up, and different refrigerants. For the tests and simulations described in this work, the selected configuration is the one represented schematically in Fig. 1. This is a simple compression cycle consisting of a compressor, a gas cooler, an IHX, a back pressure valve (BPV), a liquid receiver an electronic expansion valve (EEV) and an evaporator. Evaporator, gas cooler and IHX are brazed plate SWEP heat exchangers. The compressor is a reciprocating semi-hermetic DORIN compressor, the liquid receiver is 10 L capacity TECNAC vertical receiver and both, the BPV and the EEV are CAREL electronic valves. The BPV controls the pressure in the gas cooler, whereas the EEV controls the superheating degree at the evaporator outlet. The different components selected for the heat pump are gathered in Table 1. The geometrical characteristics of the IHX available in the experimental facility are summarized in Table 2 and are later used as comparison reference.

In the system, the simple refrigerant cycle exchanges heat with two water loops, hot and cold, respectively. The cold-water loop provides heat to the evaporator by functioning as a heat reservoir. To keep the temperature of the cold water entering the evaporator constant, a tank equipped with an electrical resistance is used. On the other hand, the hot water loop, which functions as a heat sink, receives heat from the gas cooler. The hot water is poured into a stratified tank, which can be kept at a constant temperature by means of a chiller, for stationary operation. Otherwise, the chiller can remain on standby when the tank is heating up.

The heat pump system is instrumented in order to measure refrigerant temperature, by means of high-precision resistance temperature detectors (RTD), and refrigerant pressure by means of absolute pressure transmitters, in 13 different points. The pressure drop in heat exchangers is monitored by differential pressure transmitters. Temperature and pressure are also measured at the inlets and outlets of the water loops. Also, the hot water tank is equipped with 10 different RTD to monitor temperature at different locations, evenly distributed throughout the height of the tank. This allows to observe the thermal stratification in it. The instrumentation for mass flow measurement consists of a Coriolis effect mass flow meter for the refrigerant, as well as electromagnetic flow meters for the water loops. The control of mass flow and temperature of the water in the evaporator and gas cooler loops, to ensure that the installation works in stationary mode, is carried out by four PIDs that act on the water drive pumps and 3-way valves. When the installation works in transient mode (i.e., heating tests), the controllers of the hot

Table 3
Combined standard uncertainty of the system's main variables.

Parameter	Measuring range	Absolute uncertainty	Relative uncertainty (%)
COP	2.58–7.02	±0.004–0.246	0.08–6.49
Compression work (kW)	1.10–1.66	±0.015–0.097	0.91–6.42
IHX heat transfer rate-HP side (kW)	0–2.08	±0.002–0.900	1.31–95.7
IHX heat transfer rate-LP side (kW)	0–1.80	±0.010–0.061	0.95–12.5
Evaporator heat transfer rate-refrigerant side (kW)	2.72–8.11	±0.016–0.133	0.25–3.72
Gas cooler heat transfer rate-refrigerant side (kW)	4.04–9.60	±0.016–0.342	0.22–6.46

water loop become inactive. The uncertainty analysis of the system was carried out in previous work [17] following the procedure of JCGM 100 (BIPM, IEC, IFCC and ILAC, ISO, IUPAC, 2008), in order to find the combined standard uncertainty of the main variables considered, and it is summarized in Table 3.

2.2. Numerical model and test methodology

The use of internal heat exchangers (IHX) in transcritical CO_2 heat pumps and refrigeration systems has been studied numerically [10,18], experimentally [19–21], or by a combined numerical-experimental methodology [22]. Experimental studies usually only compare system performance with and without IHX at different evaporation temperatures or different gas cooler operating conditions [19–21]. On the other hand, numerical studies typically assume different constant values for the IHX effectiveness and study its influence on system's performance. The methodology proposed for this study consists of a series of experimental heating tests in which the installation starts from an initial shutdown condition, in which both the refrigerant and the water in the hot water tank are at 10 °C and, throughout a transitory process, they heat up until a stationary is reached at the hot water set point temperature. In addition, the heat pump system is numerically analyzed, using mathematical models developed for each of the components, which allows the surface of the IHX to be varied in the model to analyze the IHX effectiveness and its influence on the system's COP.

2.2.1. Mathematical modeling of the system's components

The numerical model developed to analyze the system's behavior has been implemented in MATLAB® and validated against previously obtained experimental results [17]. Each of the components of the system has been modeled by using numerical expressions that accurately reproduce their behavior. The compressor has been modeled through its ANSI/AHRI Standard 540-2015 behavioral curves, using the correlation coefficients provided by the manufacturer, that have been adapted to match the experimental observations. Using the coefficients in Table 4, the compressor mass flow rate ($\dot{m}_c$, in kg·s^{-1}) and power rate ($\dot{W}_c$, in W) can be calculated as:

$$\dot{m}_c = C_1 + \left(\frac{\rho_a}{\rho_r}\right)\cdot\left[C_2\cdot T_{ev} + C_3\cdot P_{gc} + C_4\cdot T_{ev}^2 + C_5\cdot T_{ev}\cdot P_{gc} + C_6\cdot P_{gc}^2 + C_7\cdot T_{ev}^3 + C_8\cdot P_{gc}\cdot T_{ev}^2 + C_9\cdot T_{ev}\cdot P_{gc}^2 + C_{10}\cdot P_{gc}^3\right], \quad (1)$$

$$\dot{W}_c = C_1 + \left(\frac{\rho_a}{\rho_r}\right)\cdot\left[C_2\cdot T_{ev} + C_3\cdot P_{gc} + C_4\cdot T_{ev}^2 + C_5\cdot T_{ev}\cdot P_{gc} + C_6\cdot P_{gc}^2 + C_7\cdot T_{ev}^3 + C_8\cdot P_{gc}\cdot T_{ev}^2 + C_9\cdot T_{ev}\cdot P_{gc}^2 + C_{10}\cdot P_{gc}^3\right], \quad (2)$$

where the input variables are the discharge pressure (P_{gc}, in bar) and the evaporation temperature (T_{ev}, in Celsius), the density of the refrigerant at rated conditions (ρ_r, in kg·m^{-3}), and the density of the refrigerant at compressor suction (ρ_a, in kg·m^{-3}).

For the evaporator, gas cooler and IHX, a one-dimensional cell-by-cell discretization of each stream at the heat exchanger has been posed, that applies energy conservation equation to each control volume and solves iteratively until convergence in the heat transfer area is reached. In this installation, the heat exchangers work in countercurrent flow. As phase change can happen in them, the discretization is carried out differently in each stream depending on which one is being considered. In the case of the evaporator, the phase-changing current is discretized in n cells where the vapor quality difference is considered constant. In the superheating part, the stream is divided into another n elements where the temperature difference is considered constant. This last procedure is also applied to the gas cooler and the IHX, where there is no phase change (single phase). In the case of the evaporator, the model inputs are the mass flow rates of the fluids, the inlet enthalpies, the inlet pressure of the secondary fluid, and the superheating. Therefore, after successive iterations, the refrigerant inlet pressure, P_{ri}, is calculated. In the first iteration, P_{ri} is given an arbitrary value which is the average value of a high pressure value, P_{high}, initially equal to the saturation pressure at the inlet temperature of the secondary fluid, and a lower value, P_{low}, equal to the saturation pressure at an arbitrary temperature value (e.g. −40 °C), so, $P_{ri} = (P_{low} + P_{high})/2$. Later on, the algorithm calculates, first, the pressure drop, by means of an experimental correlation developed by Churchill [23], for single phase line, or a correlation by Chisholm [24] if there is phase change. The calculated pressure drop is used to compute, the pressure and enthalpy of the following node and heat exchanged in this cell. To calculate the enthalpies and temperatures of the secondary fluid at different nodes, it is assumed that the heat exchanged by the refrigerant is the same, with opposite sign, as that exchanged by the secondary fluid. In this methodology, local heat transfer coefficients must also be calculated for each cell. This is done by considering the average physicochemical properties of each cell when using the experimental correlations derived by Bogaert and Bölcs [25], for single phase, and by Cooper [26] for the phase-changing fluid (evaporation). Then, the heat transfer area is calculated (A_{calc}) and compared with the known area of the exchanger (A_0), so the values used to determine the inlet pressure are reassigned depending on:

$$\text{If } A_0 > A_{calc} \rightarrow P_{high} = P_{ri} \quad (3)$$

$$\text{If } A_0 < A_{calc} \rightarrow P_{low} = P_{ri} \quad (4)$$

$$P_{ri} = \frac{P_{high} + P_{low}}{2} \quad (5)$$

This serves as a convergence criterion: the process is repeated until $P_{ri} = P_{high} = P_{low}$. In heat exchangers where no phase change takes place (such as the IHX, or the gas cooler operating in a transcritical regime), the inputs are the mass flow rates and the inlet pressures and enthalpies of both fluids. Taking this into account, both streams can be discretized into n cells with equal heat exchanged. In this way, a value is given to the outlet temperature of the hot fluid at the initial iteration. This is an

Table 4
Coefficients for compressor numerical model.

	C_1	C_2	C_3	C_4	C_5	C_6	C_7	C_8	C_9	C_{10}
$\dot{m}$	0.004681	−0.002017	0.001428	$-3.2\cdot10^{-6}$	$8.45\cdot10^{-5}$	$-2.45\cdot10^{-5}$	$4.28\cdot10^{-7}$	$1.68\cdot10^{-7}$	$-5.66\cdot10^{-7}$	$1.23\cdot10^{-7}$
$\dot{W}$	966.304	−101.626	−23.414	−0.10299	1.71622	0.64412	−0.021845	−0.005984	−0.005546	−0.003224

average value of a high temperature, which is exactly the inlet temperature of the hot fluid $T_{high} = T_{hot,in}$, and the lowest value, which is the inlet temperature of the cold fluid $T_{low} = T_{cold,in}$, such that $T_{out} = (T_{high} + T_{low})/2$. With this, and assuming equal pressure in the heat exchanger for this first calculation, the outlet enthalpy of the hot fluid is estimated:

$$h_{hot,out} = \frac{h_{high} + h_{low}}{2} \tag{6}$$

Assuming equal temperature difference at each cell of the hot fluid, the pressure drop, the pressure and the enthalpy of each node are computed. As the heat exchanged by the fluids should be the same at each cell, thermodynamic variables of all nodes are calculated on the cold fluid stream. Using the experimental correlations detailed above, the local heat transfer coefficients of each cell and A_{calc} are calculated. This time, the outlet temperature of the hot fluid is re-evaluated, so depending on:

$$\text{If } A_0 < A_{calc} \rightarrow T_{high} = T_{hot,out} \tag{7}$$

$$\text{If } A_0 > A_{calc} \rightarrow T_{low} = T_{hot,out} \tag{8}$$

and the convergence criterion is: $T_{hot,out} = T_{high} = T_{low}$. Finally, both the BPV and the EEV have been modeled as isenthalpic expansion devices capable to exactly maintain the set point assigned. The liquid receiver has been treated as an adiabatic pipe that does not produce any effect (nor even pressure drop) in the system. The interested reader is referred to [27,28] where this methodology is explained in detail.

All these components have been connected in a MATLAB® model in order to analyze the influence that the size of the IHX has on system's performance at different operating conditions during domestic hot water generation using a 772 L capacity storage tank. The initial tank temperature was assumed to be 10 °C and the system operates under transient operating conditions until the temperature in the tank reaches the set point temperature of 60 °C. The EEV maintains the superheating degree at 5 K, and the BPV maintains the optimal operating pressure according to the model developed by the authors [16], through an analysis procedure based on multiple-variable regression. The value of optimal gas cooler pressure, $P_{gc,opt}$ (bar), is computed as a function of the evaporation temperature (T_{ev}, °C), the refrigerant outlet temperature in the gas cooler ($T_{gc,out}$, °C), and the temperature at the compressor outlet ($T_{c,out}$, °C) through the following linear correlations:

$$\begin{aligned}\text{If } T_{c,out} < 140^{\circ}\text{C} &\rightarrow P_{gc,opt} \\ &= \min\left(140; 11.047 + 2.2756 \cdot T_{gc,out} + 0.047279 \cdot T_{evap} - 0.20814 \cdot T_{c,in}\right)\end{aligned} \tag{9}$$

$$\begin{aligned}\text{If } T_{c,out} \geq 140^{\circ}\text{C} &\rightarrow P_{gc,opt} \\ &= \min\left(140; 140.74 + 0.031555 \cdot T_{gc,out} + 2.7227 \cdot T_{evap} - 1.0086 \cdot T_{c,in}\right)\end{aligned} \tag{10}$$

The expressions of Eqs. (9) and (10) are limited to 140 bar to ensure the integrity of the installation components against possible overpressures. For the set point temperature considered in this work of 60 °C, the value provided by the expressions is already very close to the limit. Pressure limitation is usual in refrigeration equipment and CO_2 heat pumps and many commercial systems limit the pressure to lower values (i.e., 120 bar), which allows the integration of lower cost components.

2.2.2. Test methodology

The performance of the system with and without IHX, under optimal pressure conditions, has also been experimentally evaluated. The methodology used in this study examines the transient behavior of the installation during tank water heating tests, from an initial state at 10 °C to the setpoint temperature of 60 °C. The tests have been carried out using the experimental heat pump described in Section 2, which is installed in the laboratories of Universidad Politécnica de Cartagena. To do this, the installation has manually operated valves (which, for clarity, have not been displayed in the diagram of Fig. 1) that allow the IHX to be bypassed.

The conditions imposed in the simulations are similar to those considered in the experimental tests which correspond to the conditions proposed in the stage C test defined in the EN 16147 standard [29]. For the objectives described in this work, only the test with the highest mass output is necessary, so this test is the one described in the following sections. The interested reader is referred to [30], where the experimental results are presented in detail. Consequently, in the gas cooler, the water mass flow rate has been set for a demand of 1100 kg·h^{-1}. The water inlet temperature in the evaporator has been set at 10 °C, equal to the initial temperature of the water in the tank. The water outlet temperature in the evaporator is equal to 7 °C and, to maintain these conditions, a variable water flow rate is used. The sampling rate was set between 6 and 20 s.

The theoretical thermodynamic COP of the cycle, from the point of view of the refrigerant cycle, can be calculated from the pressure and temperature measurements as:

$$\text{COP}_{\text{th,exp}} = \frac{Q_{gc}}{W_{comp}} = \frac{\frac{1}{2}\left(\dot{m}_r \Delta h_{r,gc} + \dot{m}_w \Delta h_{w,gc}\right)\Delta t}{\dot{m}_r \Delta h_{r,comp} \Delta t} \tag{11}$$

where $\Delta h_{r,gc}$ is the enthalpy change of the refrigerant in the gas cooler and $\Delta h_{w,gc}$ is the enthalpy jump of the water, while $\Delta h_{r,comp}$ is the enthalpy change of the refrigerant in the compressor. Δt is the time step corresponding to the sampling rate (20 s for the refrigerant cycle). This definition of COP has proven to be much more precise than the thermodynamic COP based solely on $\Delta h_{r,gc}$, since by taking into account the enthalpy of the water stream in the gas cooler, it partially eliminates the effect of heat losses.

However, the COP of the installation, from a practical point of view, can be calculated as the quotient between the total heat stored in the tank and the electrical energy consumed by the compressor, which are measured empirically in each test. For the heating tests, the heat supplied to the tank can be obtained from the variation of the average temperature of the tank from the initial state to the end of the experiment: $\Delta \widehat{T}_{tank} = \widehat{T}_{tank}|_{t=0} - \widehat{T}_{tank}|_{t=t_f}$. The calculation of $\widehat{T}_{tank}$ is carried out considering the temperature measurements that are made in ten different points within the tank. On the other hand, the energy consumed by the compressor is the sum of all the consumption measured every 20 s throughout the experiment. This results in what we have named the effective COP:

$$\text{COP}_{\text{eff,exp}} = \frac{Q_{tank}}{W_{elec}} = \frac{M_w c_{p,w} \Delta \widehat{T}_{tank}}{\sum \dot{W}_e \Delta t}, \tag{12}$$

where $c_{p,w}$ is the specific heat of the water (it has been considered constant and equal to 4.179 kJ·kg^{-1}·K^{-1}), $\dot{W}_e$ (kW) is the on-time measurement of electrical power consumed, Δt (s) is the time step corresponding to the sampling rate. M_w is the total mass of water contained in the tank which, according to the manufacturer's data sheet, and assuming a density of water of 1000 kg·m^{-3} is 772 kg. This effective COP gives a much more realistic account of the overall performance of the installation, including the heat accumulator, since it takes into account the mechanical losses in the compressor and the heat losses in the gas cooler and the hot water circuit.

3. Results and discussion

This section presents the results of the study, both from a numerical and an experimental point of view. First, simulations have been carried out, using the numerical model described in the previous section, in which the influence of the IHX heat exchange area on the overall efficiency of the cycle and other variables is analyzed. Secondly, an experimental study is presented focused on the transitory process in

which the heat pump is used to heat the water in a tank for domestic hot water.

3.1. Numerical results

3.1.1. Influence of the heat exchange area.

In order to analyze the influence that IHX characteristics have on the system's performance and the operating conditions, five different cases have been studied from the numerical point of view by varying the effective heat exchange area of the IHX. The heat exchange area can be increased by varying the number of plates to 8 and 16 (to get double and quadruple the original area of the exchanger). And, by decreasing the height and the width of the plates, in order to obtain half and a quarter of the original exchanging surface.

In the simulations presented below, the complete system implemented in Matlab® has been considered. It is assumed that the heat pump system is coupled to a hot water tank that is initially at a uniform temperature of 10 °C and that is warming up as a result of the heat pump operation. The numerical model simulates the water heating process during which the operating point of the installation changes. In all this transient process, the inlet water to the evaporator (that is, the heat source of the system) is considered to be at constant temperature at all times, and equal to $T_{w,evap,in} = 15$ °C. Also, the superheating temperature of the refrigerant in the evaporator, which is an input variable, has been set to a constant value of $SH = 5$ °C.

The objective is to isolate the effect of the IHX exchange area from other variables. For this purpose, the water flow rate in the gas cooler has been set constant, as well as the water flow rate in the evaporator, for a specific operating point in which $\dot{m}_{w,gc} = 500$ kg·h^{-1} and $\dot{m}_{w,evap} = 1000$ kg·h^{-1}. The mass flow of refrigerant circulating through the system varies depending on the working pressure and the gas cooler heating power.

The gas cooler pressure is initially 74 bar, and it increases as the inlet water in the gas cooler enters at higher temperature, so that the system's operating point changes and the compressor discharge temperature increases. In the same way, it is observed that the evaporation temperature and the water outlet temperature in the evaporator are progressively increasing. All this has been represented in Fig. 2, where the coefficient of performance (COP), the effectiveness of the IHX, the suction and discharge temperatures of the gas cooler and the working pressure of the gas cooler are shown, all as a function of the water inlet temperature in the gas cooler $T_{w,gc,in}$ (i.e., the return temperature from the water tank). Since simulations for five IHX exchange areas are represented, it is observed how this heat exchange area affects the represented variables.

The coefficient of performance (COP), represented in Fig. 2 (a), is defined as:

$$\mathrm{COP} = \frac{\dot{Q}_{gc}}{\dot{W}_{comp}} = \frac{\dot{m}_r\left(h_{r,gc,in} - h_{r,gc,out}\right)}{\dot{m}_r\left(h_{comp,out} - h_{comp,in}\right)} \tag{13}$$

Also, the effectiveness of the IHX, represented in Fig. 2 (b), is calculated as:

$$\varepsilon_{IHX} = \frac{\frac{\dot{Q}_{IHX}}{\dot{m}_r}}{\min\left\{\frac{\dot{Q}_{max,HP}}{\dot{m}_r}; \frac{\dot{Q}_{max,LP}}{\dot{m}_r}\right\}} = \frac{h_{r,gc,out} - h_{IHX,HP,out}}{\min\left\{h_{r,gc,out} - h_{min}\left(P_{gc}, T_{evap} + SH\right); h_{max}\left(P_{evap}, T_{gc,out}\right) - h_{evap,out}\right\}} \tag{14}$$

The heat exchanged in the IHX can be calculated both from the heat released by the high-pressure refrigerant stream $\dot{Q}_{IHX,HP}$, and that acquired by the low-pressure refrigerant $\dot{Q}_{IHX,LP}$. That is to say:

$$\dot{Q}_{IHX}/\dot{m}_r = h_{r,gc,out} - h_{IHX,HP,out} = h_{IHX,LP,out} - h_{r,evap,out} \tag{15}$$

According to Fig. 2 (a) and Fig. 2 (b), the system's efficiency clearly improves as the exchanging surface increases, being the improvement in the COP proportional to the improvement obtained in the IHX effectiveness as the exchanging surface increases. For each case studied (16 plates, 8 plates, etc.), the IHX effectiveness increments can be calculated at each moment of the transient heating process (that is, for each time, $\Delta\varepsilon = \varepsilon_x - \varepsilon_{4plates}$, where ε_x is the effectiveness for a given area). We can also calculate the increase in COP for each instant of time (that is, $\Delta\mathrm{COP} = \mathrm{COP}_x - \mathrm{COP}_{4plates}$, where COP_x is the performance coefficient for a given area). In Fig. 3, ΔCOP versus $\Delta\varepsilon$ are represented for all the

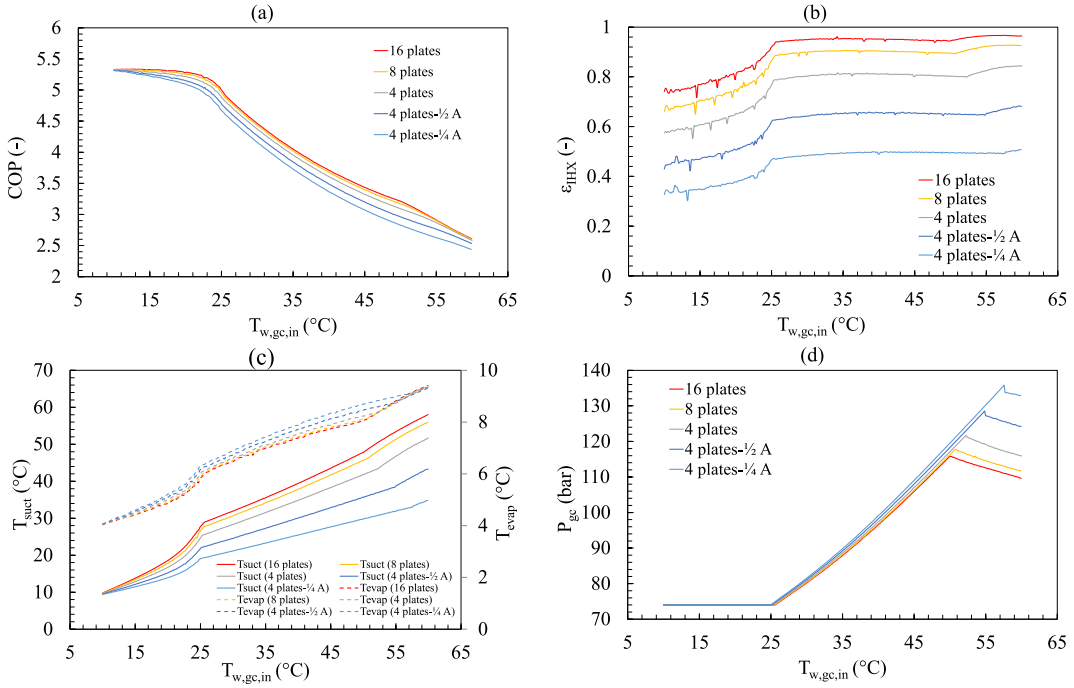

Fig. 2. Influence of IHX exchanging surface in system's performance.

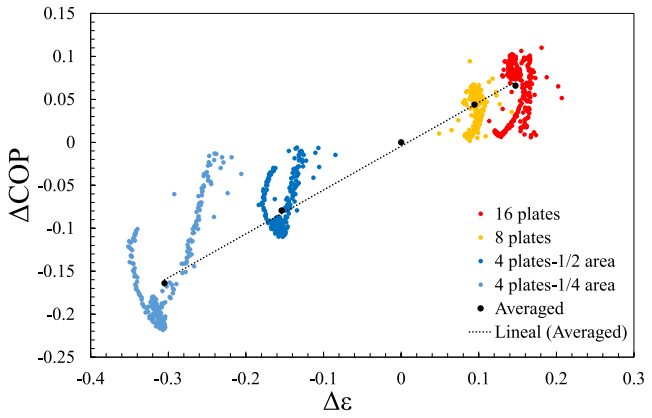

Fig. 3. Improvement in COP as a consequence of the variation of the exchanging surface, versus improvement in IHX effectiveness.

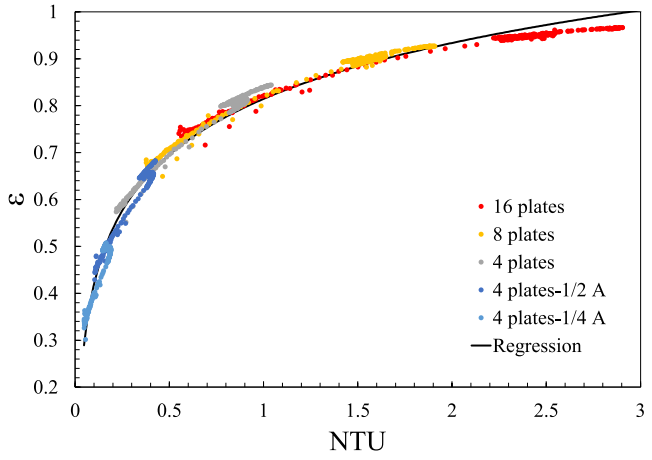

Fig. 4. Effectiveness vs. NTU for the IHX.

individual points of the transient. Also, when the averages for each case are represented (black points in Fig. 3), we find that they follow a linear correlation ($R^2 = 0.998$), in the form: $\Delta\bar{C}OP = 0.5097 \cdot \bar{\Delta\varepsilon} - 0.0046$.

It is also observed in Fig. 3 that the effect of increasing from 4 to 8 plates is greater than increasing from 8 to 16. That is, as the heat transfer area increases, the increases in effectiveness and COP are smaller, although they continue maintaining the linear trend. On the contrary, it is also observed that decreasing the heat transfer area has a drastic effect in reducing the COP of the system and, therefore, it would not be advisable.

The improvement in the IHX effectiveness produces two opposite effects. On the one hand, it produces a decrease in the enthalpy of the refrigerant at the evaporator inlet. Since the water inlet temperature and mass flow rate in this point are constant, the evaporation temperature decreases as shown in Fig. 2 (c). This causes an increase in the gas cooler optimal pressure and thus a decrease in the system's efficiency. On the other hand, it produces an increase in the temperature of the refrigerant leaving the IHX low pressure side; this effect produces a decrease in the gas cooler optimal pressure and thus an increase in the system's efficiency. Since this second effect dominates over the first, as Fig. 2 (d) shows, the gas cooler optimal pressure tends to decrease as the IHX exchange area increases and, thus, the system's efficiency increases.

Although the gas cooler optimal pressure clearly increases as the water temperature increases, when the compressor discharge temperature reaches 140 °C, the model reduces gas cooler pressure to avoid higher discharge temperatures that could damage the compressor or other components. This is easily identified in Fig. 2, as there is a change of slope in the different curves when this value is reached as the gas cooler inlet water temperature increases. As Fig. 2 (d) shows, the higher the IHX effectiveness is, the sooner this situation is reached. Another consequence is that, for the cases with greater effectiveness of the IHX (i.e., cases with greater exchange area), the maximum pressure reached in the system is lower. The maximum pressure that is reached in the case of an IHX with 16 plates is $P_{gc,max} = 115.78$ bar, while in the case with 1/4 of the original exchange area it is $P_{gc,max} = 135.79$ bar. This 20 bar difference is another important advantage, in addition to the increase in system's global COP. A reduction in working pressure generally results in a reduction of the cost of the installation, since it is more expensive to operate with components that have been certified for their use with higher working pressures. In addition, this difference in bars means that the maximum optimum pressure of the system exceeds 120 bar in the case of less effectiveness. This is remarkable, if we consider that some CO_2 heat pump manufacturers limit pressure to values around 120 bar. Precisely, the simulated case with 4 plates presents a maximum pressure of 121.71 bar, while the cases with reduced exchange area exceed that value.

In Fig. 4 the point cloud of all the simulated cases has been represented, in an effectiveness-NTU diagram of the IHX, including for each case all the intermediate states of the transient heating process. The diagram shows that the point cloud fits quite well the typical ε-NTU curve for plate heat exchangers. Together with the point cloud, a regression curve has been represented in Fig. 4 which has been adjusted to: $\varepsilon = 0.1719 \cdot \ln(\text{NTU}) + 0.8146$, with a regression coefficient $R^2 = 0.9898$. Within each simulation, for a particular heat transfer area, the effectiveness value rises as the heating process takes place. That is, as the inlet temperature of the water in the gas cooler $T_{w,gc,in}$ rises, the inlet temperature of the refrigerant on the high-pressure side of the IHX increases, and consequently does the low-pressure side refrigerant outlet temperature. This leads to an increase in the effectiveness of the IHX, as evidenced by Fig. 2 (b), in all the cases studied. However, in the ε-NTU curve (Fig. 4), the sets of points for each case follow each other, so that the configurations with a smaller exchange area are concentrated in the regions of lower NTU and minimum IHX effectiveness, while the configurations with 8 and 16 plates occupy the highest regions of the graph. It is also noticed that, in cases with a larger exchange surface, the increase in NTU is much more pronounced during heating. For example, with the 16-plate configuration, an effectiveness $\varepsilon = 0.741$ and NTU = 0.55 is obtained at the beginning ($T_{w,gc,in} = 10$ °C) and these values increase to $\varepsilon = 0.964$ and NTU = 2.84 (when $T_{w,gc,in} = 59.95$ °C), due to the considerable increase in heat transferred within the IHX.

3.1.2. *Influence of the water inlet temperature in the evaporator.*

In the results presented in the previous section, the simulations of domestic hot water heating tests have been carried out considering that the water inlet temperature to the evaporator is constant and equal to $T_{w,evap,in} = 15$ °C, as well as the superheating temperature $T_{sh} = 5$ °C. However, the temperature of the heat source undoubtedly affects the inlet and outlet temperatures of the evaporator and therefore should have some influence on the effectiveness of the IHX. In that case, the presence of IHX in the system might not be justified for some cold-water temperatures.

To analyze this effect and to confirm the suitability of the IHX regardless of the operating conditions, simulations have been carried out in which the performance of the system during the hot-water tank heating is modeled, for different temperatures $T_{w,evap,in}$, keeping the heat exchange area of the IHX constant. The base IHX with 4 plates is the model selected. Calculations begin at gas-cooler pressure $P_{gc} = 74$ bar, as the system was initially designed as a supercritical heat pump and, therefore, this study is devoted only to transcritical cycles. A lower pressure would entail the gas cooler to work in condenser mode in a subcritical cycle. Indeed, the numerical model considers that the system will work as a supercritical heat pump and, therefore, the back pressure valve will operate to always maintain the gas cooler pressure at least

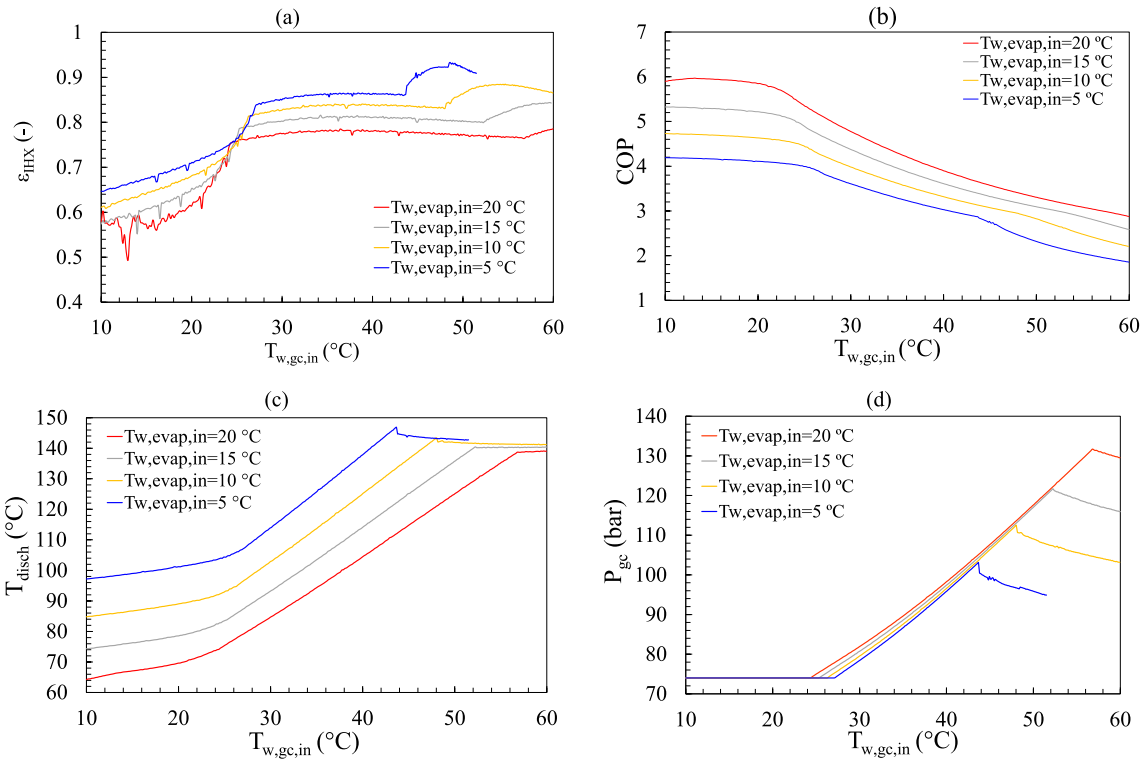

Fig. 5. Influence of water temperature at evaporator inlet on system's behavior (4 plates IHX).

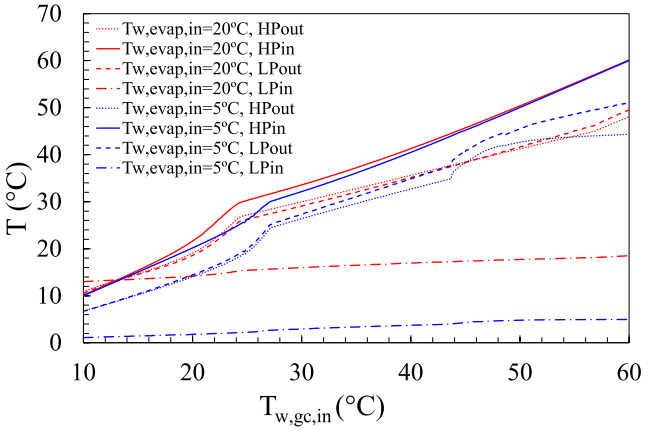

Fig. 6. Refrigerant inlet and outlet temperatures at both low- and high-pressure sides of the IHX. Results for two different evaporator water inlet temperatures.

slightly above the critical pressure.

Fig. 5 and Fig. 6 show the influence that the temperature of the water entering the evaporator has on IHX effectiveness and other parameters of the system. According to Fig. 5 (a), when the temperature difference in the IHX increases its effectiveness also increases. Four inlet water temperatures have been studied: $T_{w,evap,in}$ = 5, 10, 15, and 20 °C. The inlet water temperature in the gas cooler is $T_{w,gc,in}$ = 10 °C at the beginning and gets almost 60 °C when the tank reaches the set-point temperature. As Fig. 5 (a) shows, the sharper variation in the IHX effectiveness takes place during the initial water heating up, when the optimal gas cooler pressure (Fig. 5, d) remains stable in 74 bar, the COP is almost constant (Fig. 5, b) and the increase in water temperature is faster, as represented in Fig. 6 (note that in Fig. 6 only the two extreme evaporator water inlet temperatures have been depicted, for the sake of clarity). When pressure begins to increase during the heating process, in order to satisfy the optimal pressure condition, the COP reduces faster and the increase in water temperature is slower. This effect can be appreciated in the refrigerant inlet and outlet temperatures at both low-pressure and high-pressure sides of the IHX (Fig. 6), as well as in the gas cooler pressure plot of Fig. 5 (d). While gas cooler pressure stays stable, the effectiveness increases; when it begins to increase, the effectiveness stays almost stable; finally, when it decreases due to the limitation in compressor discharge temperature, the effectiveness increases again.

It is worth noting that the compressor discharge temperature (which is represented in Fig. 5, c) is continuously monitored by the numerical code and is limited to a maximum temperature of 140 °C (similarly to what is done by the installation's control system in order to prevent degradation of the compressor's lubricating oil). In fact, the maximum temperature recommended by the compressor supplier is 160 °C. Given the high optimum pressures (which can exceed 130 bar), it is easy for the compressor discharge temperature to exceed 175 °C. In Fig. 5 (c) it can be seen that the discharge temperature rises rapidly as the gas-cooler pressure increases. Upon reaching the maximum allowable, the numerical method, in imitation of the heat pump control system, limits the temperature, which also affects the pressure, which is thus far from the optimum pressure.

Table 5
Summary of experimental test conditions.

Test	IHX	$T_{w,evap,in}$	$T_{w,evap,out}$	$T_{tank}\|_{t_0}$	$T_{tank}\|_{t_f}$	$\dot{m}_{w,gc}$	$\dot{m}_{w,evap}$
EXP1	Yes	10 °C	7 °C	10 °C	60 °C	1100 kg·h^{-1}	Variable
EXP2	No	10 °C	7 °C	10 °C	60 °C	1100 kg·h^{-1}	Variable

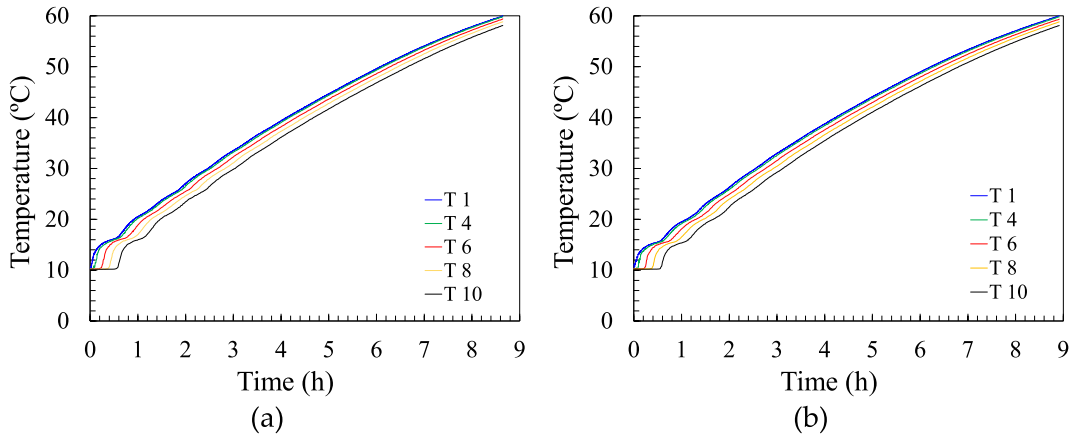

Fig. 7. Experimental results with IHX (left) and without IHX (right): Tank temperatures for EXP1 (a), and for EXP2 (b).

3.2. Experiments on the system's transient response with IHX

The transient operation of the heat pump has been evaluated, through heating tests, in accordance with the procedure and conditions detailed in Section 2.2.2. The tests allow the performance of the system to be assessed during the tank heating process, with and without IHX, from shutdown conditions, until the tank reaches the setpoint temperature of 60 °C. The results of two tests carried out under similar conditions, with and without IHX, are shown below (tests EXP1 and EXP2, respectively, in Table 5).

As shown in Table 5, in all tests the hot water flow rate in the gas cooler has been set at 1100 kg·h^{-1}. The graphs in Fig. 7 (a) and (b) show the experimental temperature variations inside the hot water tank (for clarity, only 5 of the 10 available temperature probes have been represented, T1 at the top and T10 at the bottom of the accumulator) Certain steps are observed in the initial region of the curves, which later smooth out. This is related to the way in which heat is transmitted from the upper layer of the tank to the lower layer. The hot water loop, which acts as a heat sink, exchanges heat with the DHW tank, which is normally stratified. The hot water from the gas cooler is injected into the top of the tank, while the return water is taken from the bottom, the coldest region, to favor the system's performance. In previous investigations, it was seen this staggering shown in Fig. 7 is more pronounced when the hot water flow is reduced, while it softens with higher flows, due to the increasing mixing inside the tank [30].

To allow comparison between the results with and without IHX under these conditions, Fig. 8 has comparatively represented (a) the evolution of temperatures at the top (T1) and bottom (T10) of the tank, (b) the electrical energy consumed by the compressor and received by the tank over time, (c) the measured instantaneous electric consumption of the compressor, (d) the instantaneous heat input to the DHW tank calculated by means of the temperature probes in the tank, and the system's COP (e and f). In Fig. 8 (a), we can observe that in the case without IHX (EXP2) the temperatures in the hot water tank are lower throughout the entire test. In the case with IHX (EXP1), the setpoint temperature is reached earlier and, consequently, the test takes less time (Table 6). The duration of the test can also be seen at the right ends of the curves in Fig. 8. In the configuration with IHX (EXP1) the power consumed by the compressor (accumulated) is greater at each instant than that of EXP2, but since EXP1 ends before, and since the COP is higher in the IHX configuration, the total energy consumed is 4.08 % lower in the IHX test (EXP1).

The electrical energy instantaneously consumed in the compressor (it is energy measured in the 20-s sampling period), as shown in Fig. 8 (c), increases until after 6 h of testing, when the temperature at the top of the tank is getting close to 60 °C. Let us note the final part of these curves (Fig. 8, c): the instantaneous electrical consumption in the last hours of the experiment (t > 6.5 h) shows a different trend in both cases. The use of the IHX causes the discharge temperature of the hot water to increase and the control system has to respond by lowering the gas cooler pressure. For this reason, the consumption of the compressor decreases in the conditions of EXP1.

The curves of instantaneous energy stored in the tank (Fig. 8, d) show significant noise, due to the fact that the temperature variations in the tank are very slow, so that the temperature differences between two time instants are small, of the order of the precision of the sensors, and are affected by noise. In the calculation of Q_{tank}, the mass flow rate multiplies the temperature difference. Therefore, any oscillation in the temperature measurement is amplified in the conversion to enthalpy. For clarity, the curves of energy stored in the tank (Fig. 8, d) have been filtered by means of a 10-point backward Moving Average Filter (MAF). The evolution of the COP of the system throughout the experiments has been represented in graphs (e) and (f) of Fig. 8 ($COP_{eff,exp}$ has been filtered by means of a 7-point backward MAF). The COP value is always higher at the beginning of the experiments, when the cold water enters the gas cooler, and decreases as hotter water returns. In all cases tested, it is observed that the instantaneous COP with IHX is higher than that of the simple cycle. If we look at the global COP of the experiment (Table 6), the value of $COP_{th,exp}$, calculated according to Eq. (11) is 7.55 % higher in the case with IHX, while the value of $COP_{eff,exp}$, calculated according to Eq. (12), increases by 4.26 %.

During the heating process, the system's operating point evolves from lower pressures in the gas cooler, when the temperature of the heat sink water loop is low, to transcritical values for higher temperatures. The control system developed for the heat pump allowed to easily switch from operating in subcritical mode to supercritical mode. So, in the experimental tests the system started operating under a subcritical cycle and, upon a certain water inlet temperature at the gas cooler, the system switched to a supercritical cycle. Considering the experimental COP obtained in the first moments of heating (Fig. 8, e and f), we conclude that thanks to this adaptation in the operation of the heat pump, the COP of the system is higher than the prediction given by the numerical model. In order to compare numerical and experimental results (given that the numerical study of Section 3.1 is carried out under operating conditions different from the experimental ones), a new simulation has been carried out maintaining the conditions of the experiments. The numerical COP results are compared with the experimental thermodynamic COP in Fig. 9. In the first stage of heating, the experimental COP is

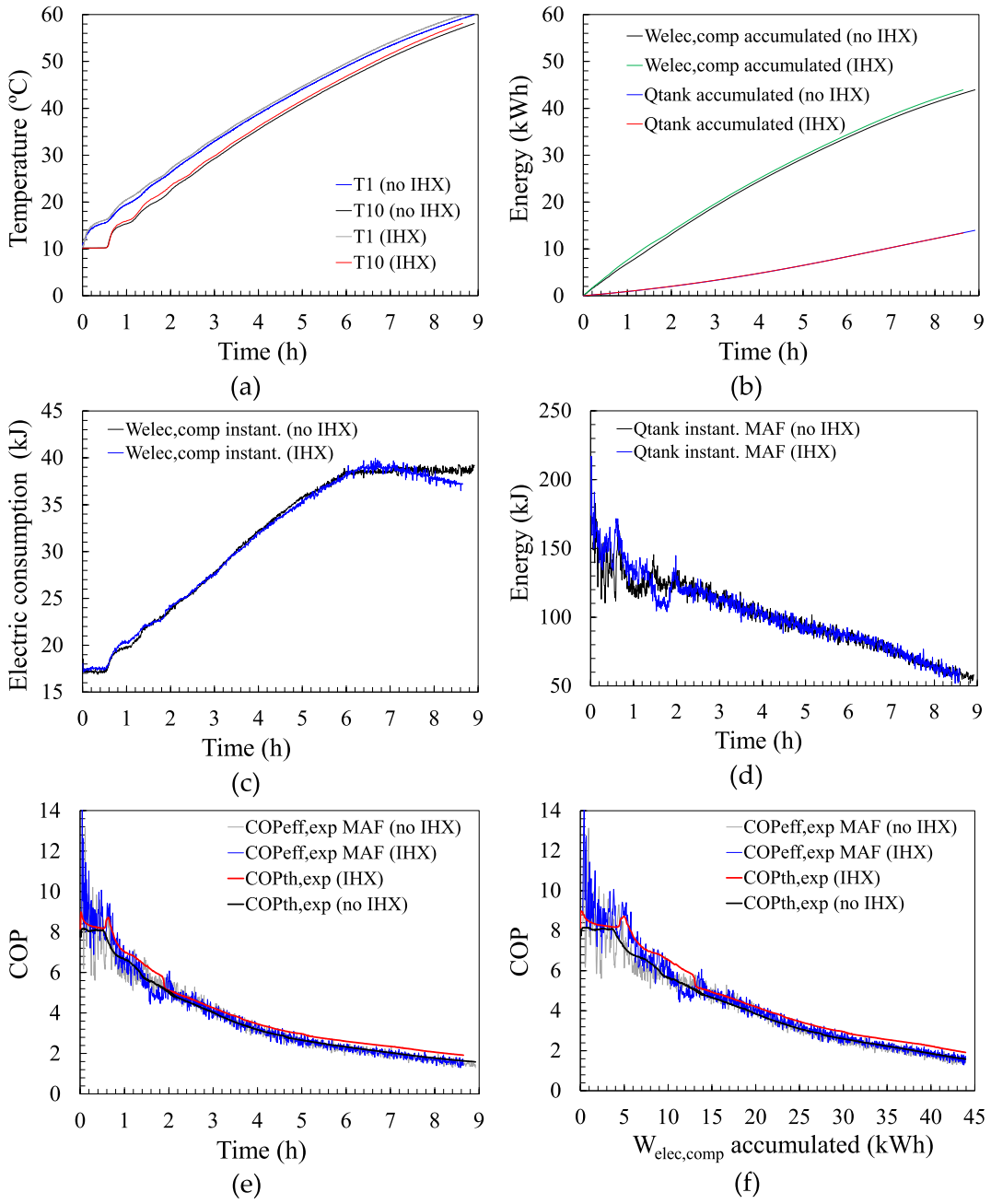

Fig. 8. Comparative experimental results with and without IHX.

Table 6
Summary of experimental results.

Test	Test time	$\Delta h_{r,comp}$ (kWh)	W_{elec} (kWh)	$\Delta h_{r,gc}$ (kWh)	$\Delta h_{w,gc}$ (kWh)	Q_{tank} (kWh)	$COP_{th,exp}$	$COP_{eff,exp}$
EXP1	8.639 h	13.1078	13.4001	46.3778	54.2833	43.9569	3.756	3.281
EXP2	8.911 h	13.6587	13.9709	43.3331	54.2508	43.9557	3.492	3.146

greater than the numerically predicted COP, since the numerical study was carried out assuming that the facility would operate always as a supercritical system during the first test stage. Once experimental tests reach supercritical pressure, around $t = 2.8$ h and water inlet temperature 29 °C, experimental and numerical results tend to converge (Fig. 9). In view of the results and the significant improvement in the COP when the system operates in subcritical conditions (when water inlet temperature at the gas cooler is low), it remains as future work to develop a numerical model for the gas cooler operating as a condenser, considering the three possible zones (superheated steam, two-phase, and subcooled liquid) and to incorporate it into the global model of the heat pump system.

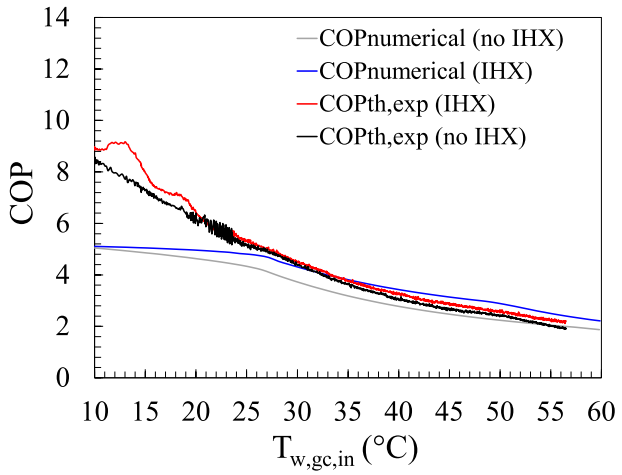

Fig. 9. Coefficient of performance (COP) for numerical simulations and thermodynamic COP for experiments with and without IHX.

Another interesting aspect to take into account is the reduction in the gas cooler maximum pressure that the use of IHX entails. In the experimental installation, in addition to the maximum temperature limitation $T_{max} = 140$ °C at the compressor discharge, which has been mentioned above, the maximum pressure has also been limited to 112 bar, as a redundant safety condition. This maximum pressure value is suitable for the heat pump working with IHX (in these conditions, the pressure of 112 bar is reached with a compressor discharge temperature of around 140 °C). This safety condition was also maintained for the test without IHX because it was considered that its influence on the results would be of little importance. To compare the pressures and temperatures with and without IHX, the compressor discharge pressure and temperature have been represented comparatively in Fig. 10. The graphs show that, in the case without IHX (EXP2), the maximum pressure reaches 112 bar and remains fixed at that value at $t = 5.97$ h, despite the fact that the discharge temperature is still relatively low (122.57 °C, reaching a maximum of 123.48 °C at $t = 6.17$ h). However, in the test with IHX (EXP1), pressure is initially maintained at 111 bar while the discharge temperature is below 140 °C and, later, it begins to decline in order to maintain the maximum temperature at that value.

4. Conclusions and future work

Through the numerical study of the transcritical CO_2 heat pump system, the analysis of the system performance with a plate heat exchanger working as IHX has been carried out. The effective exchange area of the IHX has been varied numerically (simulating five different numbers of plates) to assess the effect of the heat exchanger effectiveness on the system's COP. Transient simulations of the heating process of a DHW tank coupled to the heat pump have shown that the system's COP and the effectiveness of the IHX are directly related: COP clearly improves as the exchanging surface increases. In addition, the improvement in the COP is proportional to the improvement obtained in the IHX effectiveness as the exchanging surface increases: the increase in COP and the increase in IHX effectiveness follow a linear correlation. The greatest improvement has been achieved by growing from 4 to 8 plates in the IHX, but the COP continues to improve as the exchange area increases, for the configurations studied. Likewise, the numerical results advise against reducing the IHX area.

Simulations also show the temperature of the heat source affects the effectiveness of the IHX. Four inlet water temperatures at the evaporator have been studied to confirm the suitability of the IHX regardless of the operating conditions. The advantages of the IHX are more evident in the cases with higher temperature of the heat source but are maintained even in the cases simulated with colder water. The IHX effectiveness also varies with the temperature difference between IHX ports, increasing as evaporation temperature decreases or heated water temperature increases.

The transient heating tests carried out in the experimental transcritical heat pump (with and without IHX) coupled to a DHW tank, have shown that in the case with IHX higher temperatures in the tank are found throughout the duration of the tests, and the test duration is shorter. In the configuration with IHX the power consumed by the compressor is higher at each instant than that without IHX, but the total energy consumed in the test with IHX is 4.08 % lower. The system's COP is higher at the beginning of the experiments and decreases as water in the DHW tank warms up. Experiments show the instantaneous COP with IHX is higher than that of the simple cycle. The global thermodynamic COP, calculated for the whole experiment, is 7.55 % higher in the case with IHX, while the effective COP, according to the energy released in the DHW tank is a 4.26 % higher.

Experimental COP is higher than the prediction given by the numerical model at the first heating steps. This is because the experimental heat pump has been allowed to work in subcritical conditions when the water entering the gas cooler is cold. As future work, a numerical model

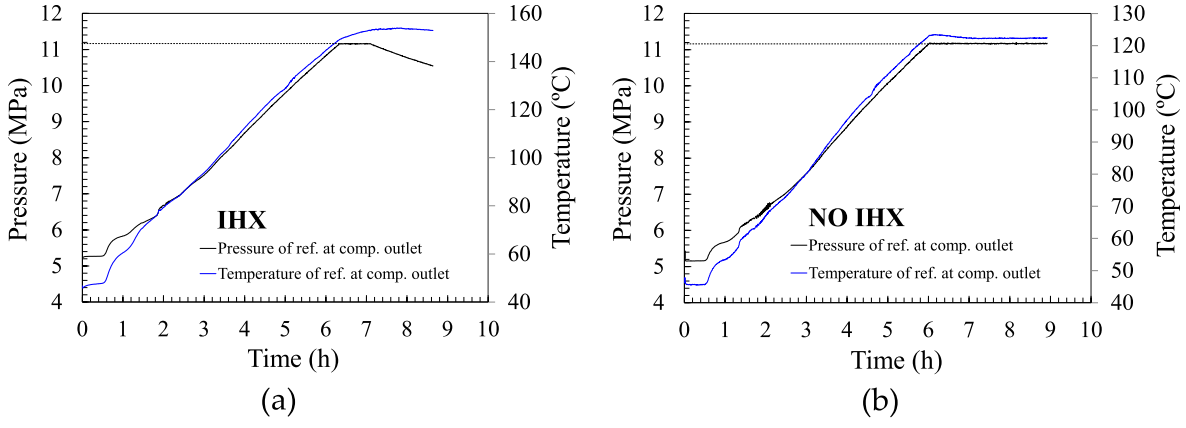

Fig. 10. Pressure and temperature at compressor outlet for experiments EXP1 (a) and EXP2 (b).

of a heat exchanger will be developed that allows it to work both as a gas cooler and as a condenser, and it will be incorporated into the global model of the system.

Funding

This work was supported by the Spanish Ministry of Economy, Industry and Competitiveness and the European Regional Development Fund through project ENE2017-83665-C2-2-P.

Declaration of Competing Interest

The authors declare that they have no known competing financial interests or personal relationships that could have appeared to influence the work reported in this paper.

Data availability

Data will be made available on request.

References

[1] G. Lorentzen, Revival of carbon dioxide as a refrigerant, Int. J. Refrig.-Revue Internationale Du Froid 17 (5) (1994) 292–301, https://doi.org/10.1016/0140-7007(94)90059-0.
[2] C. Aprea, A. Maiorino, An experimental evaluation of the transcritical CO2 refrigerator performances using an internal heat exchanger, Int. J. Refrig.-Revue Internationale Du Froid 31 (6) (2008) 1006–1011, https://doi.org/10.1016/j.ijrefrig.2007.12.016.
[3] B.T. Austin, K. Sumathy, Transcritical carbon dioxide heat pump systems: A review, Renew. Sustain. Energy Rev. 15 (8) (2011) 4013–4029, https://doi.org/10.1016/j.rser.2011.07.021.
[4] N. Fernandez, Y. Hwang, R. Radermacher, Comparison of CO2 heat pump water heater performance with baseline cycle and two high COP cycles, Int. J. Refrig.-Revue Internationale Du Froid 33 (3) (2010) 635–644, https://doi.org/10.1016/j.ijrefrig.2009.12.008.
[5] B. Dai, X. Zhao, S. Liu, Q. Yang, D. Zhong, Y. Hao, Y. Hao, Energetic, exergetic and exergoeconomic assessment of transcritical CO2 reversible system combined with dedicated mechanical subcooling (DMS) for residential heating and cooling, Energy Convers. Manage. 209 (2020) 112594, https://doi.org/10.1016/j.enconman.2020.112594.
[6] P. D'Agaro, M.A. Coppola, G. Cortella, Effect of dedicated mechanical subcooler size and gas cooler pressure control on transcritical CO2 booster systems, Appl. Therm. Eng. 182 (2021) 116145, https://doi.org/10.1016/j.applthermaleng.2020.116145.
[7] P. Aranguren, D. Sánchez, A. Casi, R. Cabello, D. Astrain, Experimental assessment of a thermoelectric subcooler included in a transcritical CO2 refrigeration plant, Appl. Therm. Eng. 190 (2021) 116826, https://doi.org/10.1016/j.applthermaleng.2021.116826.
[8] G. Lorentzen, J. Pettersen, A NEW, EFFICIENT AND ENVIRONMENTALLY BENIGN SYSTEM FOR CAR AIR-CONDITIONING, Int. J. Refrig.-Revue Internationale Du Froid 16 (1) (1993) 4–12, https://doi.org/10.1016/0140-7007(93)90014-Y.
[9] N. Calabrese, R. Mastrullo, A. Mauro, P. Rovella, M. Tammaro, Performance analysis of a rooftop, air-to-air heat pump working with CO2, Appl. Therm. Eng. 75 (2015) 1046–1054, https://doi.org/10.1016/j.applthermaleng.2014.10.057.
[10] Y. Chen, J. Gu, The optimum high pressure for CO2 transcritical refrigeration systems with internal heat exchangers, Int. J. Refrig.-Revue Internationale Du Froid 28 (8) (2005) 1238–1249, https://doi.org/10.1016/j.ijrefrig.2005.08.009.
[11] J.A. Expósito-Carrillo, F.J. Sánchez-de La Flor, B. Perís-Pérez, J.M. Salmerón-Lissén, Thermodynamic analysis of the optimal operating conditions for a two-stage CO2 refrigeration unit in warm climates with and without ejector, Appl. Therm. Eng. 185 (2021) 116284, https://doi.org/10.1016/j.applthermaleng.2020.116284.
[12] H. Cho, C. Ryu, Y. Kim, Cooling performance of a variable speed CO2 cycle with an electronic expansion valve and internal heat exchanger, Int. J. Refrig.-Revue Internationale Du Froid 30 (4) (2007) 664–671, https://doi.org/10.1016/j.ijrefrig.2006.10.004.
[13] J. Fang, X. Yin, A. Wang, X. Sun, Y. Liu, F. Cao, Cooling performance enhancement for the automobile transcritical CO2 air conditioning system with various internal heat exchanger effectiveness, Appl. Therm. Eng. 196 (2021) 117274, https://doi.org/10.1016/j.applthermaleng.2021.117274.
[14] Y. Wang, Z. Ye, X. Yin, Y. Song, F. Cao, Energy, exergy and exergoeconomic evaluation of the air source transcritical CO2 heat pump with internal heat exchanger for space heating, Int. J. Refrig 130 (2021) 14–26.
[15] S.G. Kim, Y.J. Kim, G. Lee, M.S. Kim, The performance of a transcritical CO2 cycle with an internal heat exchanger for hot water heating, Int. J. Refrig.-Revue Internationale Du Froid 28 (7) (2005) 1064–1072, https://doi.org/10.1016/j.ijrefrig.2005.03.004.
[16] F. Illán-Gómez, V.F. Sena-Cuevas, J.R. García-Cascales, F.J.S. Velasco, Analysis of the optimal gas cooler pressure of a CO2 heat pump with gas bypass for hot water generation, Appl. Therm. Eng. 182 (2021) 116110, https://doi.org/10.1016/j.applthermaleng.2020.116110.
[17] F. Illán-Gómez, V.F. Sena-Cuevas, J.R. García-Cascales, F.J.S. Velasco, Experimental and numerical study of a CO2 water-to-water heat pump for hot water generation, Int. J. Refrig 132 (2021) 30–44, https://doi.org/10.1016/j.ijrefrig.2021.09.020.
[18] L. Shao, Z. Zhang, C. Zhang, Constrained optimal high pressure equation of CO2 transcritical cycle, Appl. Therm. Eng. 128 (2018) 173–178, https://doi.org/10.1016/j.applthermaleng.2017.09.023.
[19] E. Torrella, D. Sánchez, R. Llopis, R. Cabello, Energetic evaluation of an internal heat exchanger in a CO2 transcritical refrigeration plant using experimental data, Int. J. Refrig.-Revue Internationale Du Froid 34 (1) (2011) 40–49, https://doi.org/10.1016/j.ijrefrig.2010.07.006.
[20] Y. Jiang, Y. Ma, M. Li, L. Fu, An experimental study of trans-critical CO2 water-water heat pump using compact tube-in-tube heat exchangers, Energy Convers. Manage. 76 (2013) 92–100, https://doi.org/10.1016/j.enconman.2013.07.031.
[21] F. Cao, Z. Ye, Y. Wang, Experimental investigation on the influence of internal heat exchanger in a transcritical CO2 heat pump water heater, Appl. Therm. Eng. 168 (2020) 114855, https://doi.org/10.1016/j.applthermaleng.2019.114855.
[22] F. Cao, Y. Wang, Z. Ye, Theoretical analysis of internal heat exchanger in transcritical CO2 heat pump systems and its experimental verification, Int. J. Refrig.-Revue Internationale Du Froid 106 (2019) 506–516, https://doi.org/10.1016/j.ijrefrig.2019.05.022.
[23] S. Churchill, Friction-factor equation spans all fluid-flow regimes. Chem. Eng. 84 (1977) 91-92.
[24] D. Chisholm, A. Wanniarachchi, Layout of plate heat exchangers, in: Proceedings of the ASME/JSME Thermal Engineering Proceedings, New York, 1991, pp. 433-438.
[25] R. Bogaert, A. Böles, Global performance of a prototype brazed plate heat exchanger in a large Reynolds number range, Exp. Heat Transfer 8 (4) (1995) 293–311, https://doi.org/10.1080/08916159508946508.
[26] M.G. Cooper, Heat flow rates in saturated nucleate pool boiling, Adv. Heat Transf. 16 (1984) 157–239.
[27] J.R. García-Cascales, R. Molina-Valverde, F. Illán, F.J.S. Velasco, A discretisation method for the characterisation of a plate heat exchanger working as evaporator; Published online in https://www.researchgate.net/publication/360412495, May 2022.
[28] F. Illán-Gómez, J.R. García-Cascales, R. Molina-Valverde, F.J.S. Velasco, A discretization method for the transient characterization of a plate heat exchanger working as evaporator, submitted to the Int. J. Therm. Sci. (2022).
[29] European Committee for Standardization (ECS) EN 16147, heat pump with electrically driven compressor testing, performance rating and requirements for making of domestic hot water units. **December, 2017**.
[30] F.J.S. Velasco, M.R. Haddouche, F. Illán-Gómez, J.R. García-Cascales, Experimental characterization of the coupling and heating performance of a CO2 water-to-water heat pump and a water storage tank for domestic hot water production system, Energy Build. 265 (2022) 112085, https://doi.org/10.1016/j.enbuild.2022.112085.